Landslides (2016) 13:589–601
DOI 10.1007/s10346-016-0704-8
Received: 30 October 2015
Accepted: 17 March 2016
Published online: 30 March 2016

Jia-wen Zhou · Fu-gang Xu · Xing-guo Yang · Yu-chuan Yang · Peng-yuan Lu

Comprehensive analyses of the initiation and landslide-generated wave processes of the 24 June 2015 Hongyanzi landslide at the Three Gorges Reservoir, China

Abstract Reservoir landslides pose a great threat to shipping safety, human lives and properties, and the operation of the hydropower station. In this paper, the 24 June 2015 Hongyanzi landslide at the Three Gorges Reservoir is considered as an example to study the initiation mechanism and landslide-generated wave process of a reservoir landslide. The finite difference method and limit equilibrium analysis are used to analyze the deformation and failure characteristics of the Hongyanzi slope. Simulation results show that a large deformation (about 358 mm) happens in the shallow deposits under intermittent rainfall condition, and the slope is in a limit state. At the same time, continuous rapid drawdown of the water level (about −0.55 m/day during 8–24 June 2015) reduced the support and accelerated the drainage of the water for the bank slope. A coupling effect of intermittent rainfall and rapid drawdown of the water level was the triggering factor of the 24 June Hongyanzi landslide. Landslide-generated wave process was simulated using a fluid–solid coupling method by integrating the general moving object collision model. Simulation results show that the landslide-generated wave is dominated by the impulse wave, which is generated by sliding masses entering the river with high speed. The maximum wave height is about 5.90 m, and the wave would decay gradually as it spreads because of friction and energy dissipation. To prevent reservoir landslides, the speed for the rising or drawdown of the water level should be controlled, and most importantly, rapid drawdown should be avoided.

Keywords Hongyanzi landslide · Triggering mechanism · Fluctuation of water level · Landslide-generated wave · Fluid–solid coupling model

Introduction

The Yangtze River is the mother river of China, which is characterized by a large water discharge, and it is very important because it delivers sediment and supports the lives of Chinese people (Saito et al. 2001; He et al. 2008). In recent years, due to increasing demand on the energy supply, irrigation, and flood control from the government departments, several water conservancy projects have been constructed along the Yangtze River, such as a flood protection embankment and a reservoir dam (Wu et al. 2004). The construction of high dam on a river causes the water level to rise and forms a huge reservoir upstream, which may lead changes in local climate and the ecological environment (Yin and Li 2001). Among these changes, sediment accumulation and reservoir landslides are two key issues for the Three Gorges Reservoir (Liu et al. 2004; Huang et al. 2014). Several years of observational data show that the frequency of landslides has significantly increased since the impoundment of the Three Gorges Reservoir, especially for the Three Gorges area extending from Yichang to Chongqing along the Yangtze River (Wu et al. 2004; Tang et al. 2015). These landslides pose a great threat for shipping safety, and they endanger human lives and properties and threaten the operation of the hydropower station.

Numerous catastrophic landslide events have occurred at the Three Gorges Reservoir in recent years. For example, on 12 June 1985, the Xintan landslide, with a volume of approximately 3.0×10^7 m^3, occurred 27 km away from the Sandouping dam site of the Three Gorges project. Sliding masses rushed into the river and caused a wave with a height of 80 m (He et al. 2010). On 14 July 2003, the Qianjiangping landslide, with a volume of about 2.4×10^7 m^3, occurred on the western side of the Qinggan River (a tributary of the Yangtze) and caused a wave with a height of 20 m. It resulted in 15 death and 9 missing people, and it destroyed 4 corporations and 80 houses (Wang et al. 2004; Yin et al. 2015). On 2 September 2014, the Shanshucao landslide, with a volume of 4×10^7 m^3, occurred on the left bank of the Luogudong River (a tributary of the Yangtze) and caused damage to 20 ha of citrus orchard and 27 utility poles, which resulted in direct economic losses of 5.19 million US dollars (Huang et al. 2014). Previous studies show that heavy rainfall and increasing water level are the two triggering factors for these catastrophic landslides (He et al. 2010; Jiang et al. 2015). The threat to life and property comes not only from the landslide itself but also from the landslide-generated wave, which causes huge volumes of sliding mass to rush into the river (Yin et al. 2012). Therefore, studying the triggering conditions and mechanism of landslide-generated waves and other related problems is very important for hazard prevention and mitigation of reservoir landslides.

For reservoir landslides, statistical analyses, field investigations, physical modeling tests, and numerical simulations are always used to study the triggering factors and mechanism (Guzzetti et al. 1999; Bosa and Petti 2011; Zhou et al. 2010). Statistical analyses are generally used to study the relationships between rainfall intensity/duration and landslide density, the fluctuation of water level and landslide frequency, and other factors in a specific region, and these provide the reference triggering conditions for the reservoir landslides, such as critical rainfall intensity, rising drawdown rate of the water level, and other factors (Aleotti and Chowdhury 1999; Chung and Fabbri 1999). The triggering mechanism and mass movement process of a landslide may leave behind landslide traces or deposits, so field investigations are important for studying landslides. Numerical simulation can be used to reproduce the triggering mechanism or dynamic process of a landslide. However, in most cases, using different research methods at the same time is more effective for studying the triggering mechanism or dynamic process of a landslide (Iverson

2000; Huang et al. 2014). Duc (2013) studied the rainfall-triggered large landslides on 15 December 2005 in Van Canh District through field investigations and laboratory tests, and they found that the triggering factor for this landslide was heavy rainfall. The slope stability was related to slope inclination and the thickness of the residual soils in the area. Zhang et al. (2012) used laboratory tests and numerical simulations to study the triggering mechanism of a reservoir landslide and found that water absorption/dissolution may cause a reduction in shear strength of rock masses during impoundment; this results in the initiation of a landslide.

When the sliding masses of a reservoir landslide suddenly rush into the river, a wave will be generated and will pose a great threat to the surrounding residents and their buildings and ships (Chopakatla et al. 2008; Hu et al. 2015). However, the landslide-generated wave process is very short. Observation data is often not collected, and we can only presume the details of the disaster process by using water traces and reports given by local witnesses (Koo and Kim 2008). For landslide-generated wave problems, theoretical analyses are difficult due to strong non-linearities, three-dimensional topography, and flow turbulence (Fritz et al. 2004; Abadie et al. 2010; Yin et al. 2015), and laboratory tests are limited by scale effects (Xu et al. 2015a). Therefore, numerical simulation is more reasonable for studying the dynamic process of a landslide-generated wave (Ataie-Ashtiani and Mansour-Rezaei 2009; Yavari-Ramshe and Ataie-Ashtiani 2015). For example, Yin et al. (2012) conducted a physical modeling test to study the characteristics and evolution of a landslide-generated wave, and they confirmed the presence of a head wave and determined the calculation formulas for prediction of a landslide-generated wave in the Three Gorges Reservoir area. Xu et al. (2015b) conducted a large-scale physical modeling test to study the impact of a landslide-generated wave, and they found that the contact area, landslide volume, and drop height are the main factors that effect the scale of a wave. Choi et al. (2008) conducted a 3D solitary wave run-up analysis with the Reynolds average numerical simulation (RANS) turbulent model to study the dynamics of a landslide-generated wave. Das et al. (2009) studied the impact of slide deformation and geometry on surface waves generated by submarine landslides using a computational model based on Navier–Stokes equations. Montagna et al. (2011) presented a numerical method based on the volume of fluid (VOF) technique to study tsunamis generated by the landslides falling along the flank of a conical island.

In this paper, the 24 June 2015 Hongyanzi landslide at the Three Gorges Reservoir is taken as an example to study the initiation mechanism and landslide-generated wave process of a reservoir landslide. The initiation mechanism of this landslide is studied by using field investigations, laboratory tests, numerical simulations, and theoretical analyses. A fluid–solid coupling method that integrates the general moving object (GMO) collision model is used to simulate the dynamic process of the landslide-generated wave. The initiation mechanism of the reservoir landslide and forecasting of the landslide-generated wave are discussed. The presented conclusions are useful for understanding the initiation mechanism and landslide-generated wave process of a reservoir landslide.

The Hongyanzi landslide

In this section, the hazard of the Hongyanzi landslide at the Three Gorges Reservoir is briefly introduced. Then, the geomorphology and geological conditions for the study area are described. In addition, the several years of observation data for the hydrological and climate conditions are illustrated.

Hazard overview

At 18:40, 24 June 2015, the Hongyanzi landslide (109° 53′ 40.57″ E, 31° 04′ 28.72″ N) occurred suddenly at the left bank of the Daning River in the Three Gorges Reservoir, Wushan County, Chongqing, southwest China. Figure 1 shows the location of the Hongyanzi landslide. The Hongyanzi landslide occurred on the opposite side of the Wushan wharf, about 170 km away from the dam site of the Three Gorges hydropower station. As shown in Fig. 1b, the landslide happened near the intersection of the Daning River and the Yangtze River. The river width is about 1300 m, and some residents are scattered in the mountainous area. The landslide happened in the shallow deposits, at an elevation of 120–280 m.

After the landslide was initiated, a large volume of sliding mass suddenly rushed into the Daning River and caused a wave. According to the descriptions of witnesses, the height of the landslide-generated wave was about 5.0–6.0 m. Sewage was generated by the wave at the opposite bank. As shown in Fig. 2, 13 fishing boats (including a cruise boat of 14 m) are knocked over by the landslide-generated wave. There were two deaths and six people injured. According to official data, the volume of the landslide was 2.3×10^5 m^3, and it caused the relocation of 196 people on the slope. There were economic losses of about 5 million China Yuan.

Field investigations were carried out shortly after the landslide occurred. Figure 3 shows a frontal view of the Hongyanzi landslide and the preparation of three-dimensional laser scanning works. The maximum elevation of the slope is about 350 m, and the elevation of the water surface is about 145 m. The lowest elevation of the riverbed is about 76 m. The elevation of the landslide topper was about 276 m, and the elevation of the landslide toe was about 125 m. Part of the landslide was below the water surface; the total height above the water surface was about 131 m.

Three-dimensional geometric information about the landslide itself and the surrounding terrain were obtained by using the Optech ILRIS-3D laser scanner, which was provided by the Teledyne Optech Company, Canada. Figure 4a shows a 3D point cloud of the Hongyanzi landslide. The following numerical models were used for stability analysis and simulation of the landslide-generated wave based on the measured data. Figure 4b shows a 3D visualization of the Hongyanzi landslide. The measured results show that the flat distribution area of the Hongyanzi landslide was about 3.75×10^4 m^2, the landslide volume was about 2.25×10^5 m^3, and the average thickness was about 12 m. After the landslide event of the 24 June 2015 landslide, a large amount of residual landslide deposits are still accumulated on the slope, which may cause a second landslide under heavy rainfall conditions. To avoid this, an artificial impermeable layer was used to prevent rainfall from infiltrating the slope in the current stage (as shown in Fig. 3). Moreover, some engineering measures should be also undertaken.

Geomorphology and geological conditions

The study area is crossed by several faults and rivers (such as the Yangtze River, Daning River, and Baolong River), which belong to

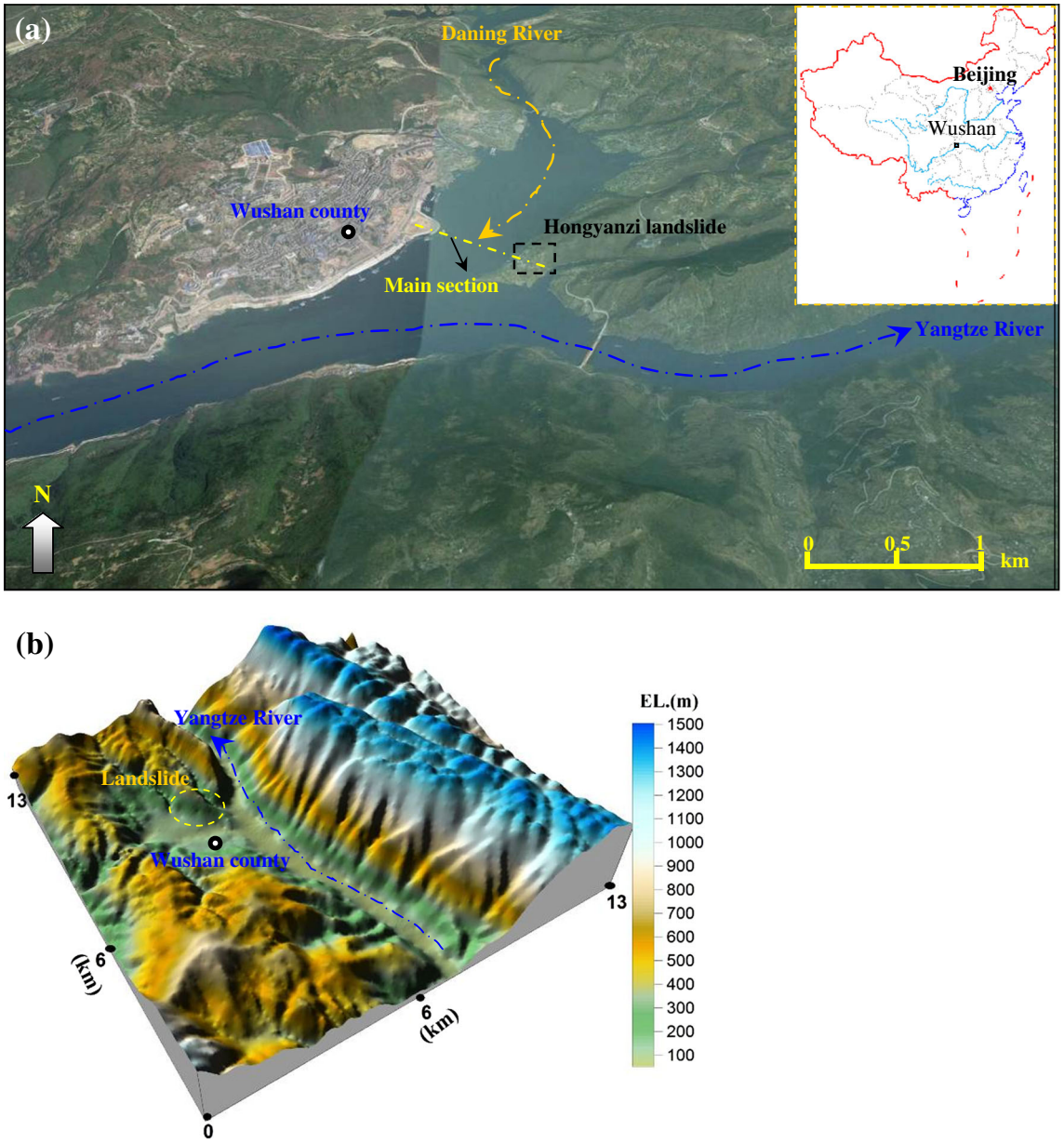

Fig. 1 Location of the Hongyanzi landslide, **a** remote sensing image and **b** three-dimensional visualization of the study area

the middle and shallow cutting fold. Mountains with steep slopes and different heights are present; most of the slopes are greater than 30°, as shown in Fig. 1b. The elevation in this area ranges from 150 to 1200 m, with strong tectonic effects. Figure 5 shows the topographical conditions for the main section (as shown in Fig. 1a) of the Hongyanzi landslide. As shown in Fig. 5, the Daning River at the entrance of the Yangtze is very wide, about 1450 m. The dip direction of the Hongyanzi slope is 308°, with an inclination of 38°–55°.

The exposed strata in this area are sedimentary rocks, and they mainly include limestone, silty limestone, mudstone, and sandstone. Quaternary sediments are well developed in this area and mainly include alluvium, diluvian, colluviums, and landslide deposits. The structural shallow deposits are loose with low shear strength, and the shallow rock masses are fractured and strongly weathered. The Hongyanzi landslide happened in the shallow slope deposits, which are mainly composed of gravel soil and silty clay with gravel (as shown in Fig. 6a), with a density of approximately 1.85–1.95 g/cm^3. The bedrock is muddy limestone and limestone. Figure 6b shows the particle size distribution characteristics for three test samples of the landslide soil. As shown in Fig. 6b, the shallow deposits are well graded with loose structure, 35 % of the particles have diameters less than 5 mm, and 10 % of particles have diameters greater than 60 mm. Table 1 summarizes the mechanical parameters for the main geomaterials of the slope after laboratory tests and engineering experience comparisons. As shown in Table 1, the deformation and strength parameters of the shallow deposits are sensitive to the water content. The shear

Fig. 2 Photos of the Hongyanzi landslide site, showing fishing boats damaged by the landslide-generated wave

strength parameters and deformation parameters all decrease with increasing water content.

Hydrological and climate conditions

The Yangtze River extends 6397 km with a total catchment area of 1.8×10^6 km². It is the largest river in China and the third largest river in the world, after the Nile and Amazon. The Yangtze River system is extensive, with more than 7000 tributaries. The main tributaries are the Yalong River, Min River, Jialin River, Wu River, and Xiang River. The average flow of the Yangtze River is 3.1×10^4 m³/s, with significant seasonal fluctuations. The flow has a great impact on the stability of the slopes on both sides.

The study area has a subtropical monsoon humid climate. It shows apparent three-dimensional climate characteristics with relatively little rain in the mountain valley and heavy rain in the mountainous area. Figure 7 shows several years of rainfall monitoring data from one of the meteorological observation points (30 km away from Wushan County (downstream), with an elevation of 299.8 m; 109° 31′ 48″ E, 31° 01′ 12″ N). In this area, the climate is moderate, with an average temperature of 18.4 °C, and rainfall is abundant with annual rainfall of 950–1200 mm. The rain

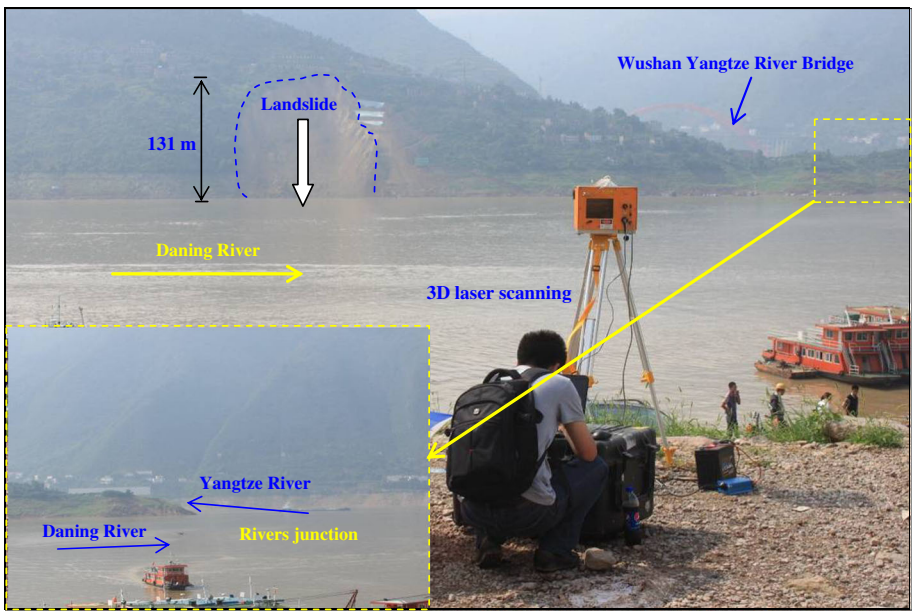

Fig. 3 Front view of the Hongyanzi landslide and setup of the three-dimensional laser scanning system

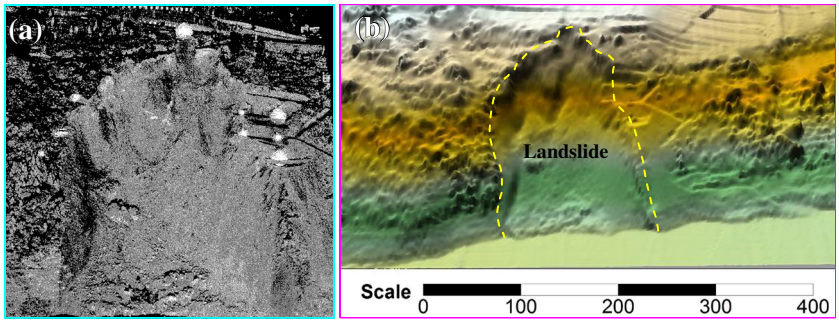

Fig. 4 Three-dimensional (3D) laser scanning results for the Hongyanzi landslide, **a** 3D point cloud of the landslide and **b** 3D visualization of the landslide (unit, m)

is concentrated between April and September. Historical monitoring data show that the maximum daily rainfall in the region can reach 90–100 mm. For example, 94.9 mm of daily rainfall occurred on 23 June 2011, 81.7 mm of daily rainfall occurred on 20 June 2008, and 81.0 mm of daily rainfall occurred on 20 June 2009. These special hydrological and climate conditions have a great impact on the occurrence frequency of reservoir landslides in the area.

Landslide initiation mechanism

In this section, the deformation and failure characteristics of the Hongyanzi slope are analyzed by using a finite difference method, and the potential slip surface is determined through numerical simulation and limit equilibrium analysis. Initiation process and mechanism of the Hongyanzi landslide are analyzed from the simulation results; the field investigations for the landslide; and the monitoring data of slope deformation, rainfall, and fluctuation of the reservoir water level.

Slope deformation and failure analyses

Finite element methods and finite difference methods have been widely used to simulate the stress and deformation of slopes and to assess slope stability (Aleotti and Chowdhury 1999; Liu et al. 2004). Here, the finite difference method is used to simulate the stress, deformation, and failure characteristics of the Hongyanzi slope. A two-dimensional (2D) problem is considered for the Hongyanzi slope. The geometry and geological conditions of the slope are shown in Fig. 8a. The 2D numerical mesh is shown in Fig. 8b; it includes 2738 nodes and 1279 elements. The Mohr-Coulomb model is used to simulate the slope strength, including shallow deposits and bedrocks. Moreover, rainfall infiltration is not directly simulated by the numerical method, where the slope soils are assumed to reach saturation under rainfall condition. The saturated soil has a lower shear strength parameters and elastic modulus than natural soil and has been reported in several previous studies (Yin et al. 2012; Zhou et al. 2013, 2016b). All of the mechanical parameters used for the simulation of the Hongyanzi slope are shown in Table 1.

Simulation results show that the stress of the Hongyanzi slope is dominated by compressive stress. The maximum first principal stress is about 6.0 MPa under continuous rainfall condition, and no tensile stress exists in the slope (as shown in Fig. 9a). The deformation of the slope is relatively small under normal conditions. The maximum horizontal displacement is 19.0 mm, and the maximum vertical displacement is 13.6 mm. However, when the shallow deposits are basically saturated under antecedent intermittent rainfall condition, the deformation of the slope sharply increases, and a large deformation occurs in the shallow deposits. As shown in Fig. 9b, the maximum deformation of the Hongyanzi slope is about 358 mm and occurs at the topper slope. The field monitoring results show that the maximum horizontal displacement of the Hongyanzi slope is about 288 mm, which is close to the simulated horizontal displacement (261 mm). Both simulated results and monitoring data show that the intermittent rainfall before the landslide resulted in large deformation of the Hongyanzi slope. Figure 9c shows the distribution characteristics for the plastic zone of the slope. The failures of the shallow deposits are all shear type, but they are not fully connected with each other. This indicates that no landslide may occur only due to rainfall, even though it causes large deformation along the shallow deposits. The shear strain increment of the slope indicates that the slope is in a limit state (Fig. 9d), and a clear potential slip surface is basically formed in the Hongyanzi slope.

The safety factor of the slope is determined by the Mongenstern-Price method (a type of limit equilibrium method) under natural and saturated conditions. Figure 10a shows the simulated results of the critical slip surface and the corresponding safety factor of the Hongyanzi slope under natural and saturated conditions. As shown in Fig. 10a, the

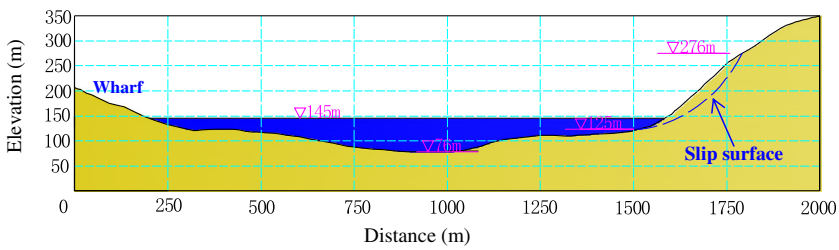

Fig. 5 Topographical conditions for the main section (Fig. 1a) of the Hongyanzi landslide

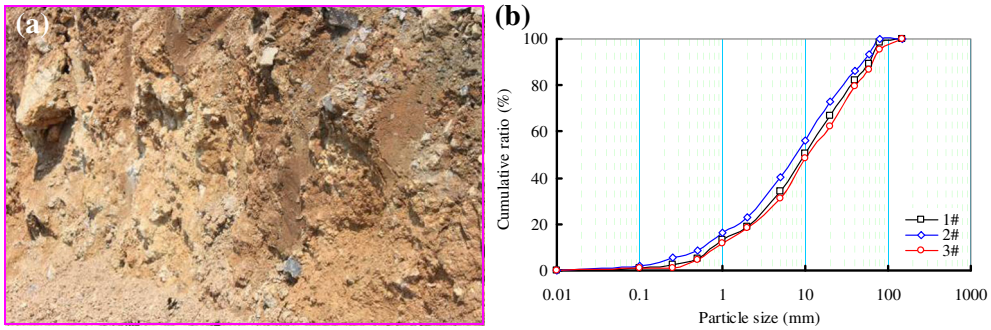

Fig. 6 Material composition and structural characteristics of the landslide soil, **a** site photo and **b** test results for particle size distribution

safety factor of the Hongyanzi slope under natural condition is 1.230 and it decreases to 1.031 under saturated condition. Simulated results mean that the slope reaches the limit state after antecedent intermittent rainfall duration. The location of the critical slip surface under rainfall condition is the same as the natural condition, which agrees with the simulated results for shear strain increment and the plastic zone of this slope obtained by using the finite difference method. Furthermore, the simulated critical slip surface is close to the post-landslide topography, but it has a certain difference at the upper slope, where the simulated landslide depth is larger than the actual depth (Fig. 10a).

Initiation process and mechanism

June is the rainy season for the study area. The daily rainfall values were 57.5 and 44.5 mm on 16 and 17 June 2015, respectively, and the daily rainfall was 4.5 mm on 20 June 2015. Before the catastrophic landslide on 24 June 2015, there was antecedent intermittent rainfall for about a week. Field monitoring results show that on 21 June 2015, a tensile fracture formed at the rear (elevation 276 m) of the Hongyanzi slope and a small slide occurred at the slope toe. On 23 June 2015, a slide occurred with a volume of 1.5×10^4 m^3 below the elevation of 175 m. Unfortunately, the deformation of the slope rear increased suddenly on the morning of 24 June 2015, and the arc shape of the tensile fracture was extended to 25–80 m, with a width of 3–10 cm. Monitoring results show that the maximum horizontal displacement of the Hongyanzi slope was about 13 cm at 13:30 on 24 June 2015. At 18:40 on the same day, a catastrophic landslide occurred in the Hongyanzi slope, with a volume of 2.3×10^5 m^3. The deformation and failure of the Hongyanzi slope were related to the intermittent rainfall and fluctuation of the water level in the Three Gorges Reservoir.

The intermittent rainfall duration resulted in the gradually saturation of shallow deposits and caused the decreasing of shear strength in the soil and increasing of pore water pressure in the slope (Iverson 2000; Zhou et al. 2016a). The deformation parameters of the shallow deposit also decreased with the increasing water content (Wu et al. 2004). Figure 11a shows the intermittent rainfall effect on the shallow deposit slope. Long-term intermittent rainfall duration made the slope soil gradually saturated and caused the decreasing of slope stability (safety factor of 1.230 under natural condition decreased to 1.031 under saturated condition). The decreasing of shear strength of soils, increasing of soil weight, and pore water pressure in the slope caused the large deformation and resulted in the limit state of the slope, but the catastrophic landslide on 24 June 2015 was not only affected by the antecedent intermittent rainfall duration. Another key factor was the fluctuation of the water level in the Three Gorges Reservoir during the same period. As shown in Fig. 10b, from 8 June 2015 to 24 June 2015, the water level of the Three Gorges rapidly declined at about −0.55 m/day. The rapid drawdown of the water level reduced the support for the Hongyanzi slope and accelerated the drainage of water in the slope, causing the internal stress of the slope to change (Fig. 11b), which lead the further decreasing of safety factor of slope and resulted in the final initiation of landslide. The initiation of the Hongyanzi landslide was the joint result of intermittent rainfall and rapid drawdown of the water level for the reservoir deposit slope.

Simulation of landslide-generated wave

Once the large volume of sliding mass rushed into the river, a wave was generated and it disturbed the balance of the river flow. Here, a numerical method is used to reproduce the dynamic process of the landslide-generated wave.

Numerical model

According to the dynamic process for the landslide-generated wave of the Hongyanzi landslide, a 3D computational fluid dynamics (CFD) code was used to solve the Reynolds-averaged Navier–Stokes equations, and the continuity equation for incompressible flow along with the true VOF method was used to

Table 1 Mechanical parameters for the main geomaterials of the slope obtained by laboratory tests and engineering experience

Type	Condition	Density (g/cm^3)	Shear strength parameters		Elastic modulus (GPa)	Poisson's ratio
			Cohesion (kPa)	Friction angle (°)		
Gravel soil	Natural	1.95	46.0	30.0	0.30	0.30
	Saturated	2.10	35.0	27.0	0.24	0.32
Limestone	Natural	2.40	800.0	40.0	3.00	0.26

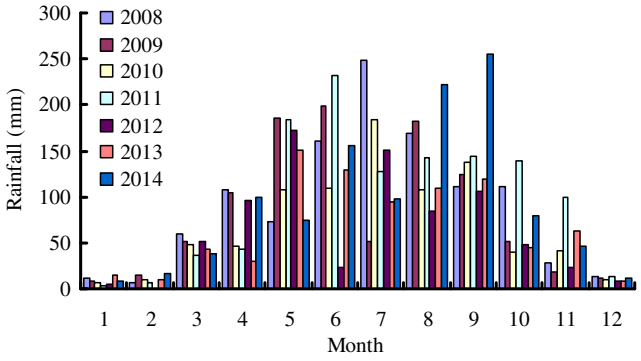

Fig. 7 Several years of rainfall monitoring data from one meteorological observation point downstream (30 km away from Wushan County)

compute the free surface motion (Montagna et al. 2011). A GMO collision model was used to simulate the sliding mass, which was represented as a rigid body under any type of physical motion (Pastor et al. 2009). The GMO collision model is suited for either being dynamically coupled with fluid flow or user-prescribed. It has six degrees of freedom to move or rotate with a fixed point or a fixed axis. The collision model includes collision detection and collision integration. The energy loss of the collision was controlled by the coefficient of restitution. Here, the motion of sliding masses is coupled with the water flow, and the sliding masses were assumed to have GMO rotary motion and collision. The overall restitution coefficient was 0, and the overall friction coefficient was 1.73, based on the characteristics of the Hongyanzi landslide and previous experience (Yin et al. 2015). The renormalization group (RNG) turbulent model was used to simulate the fluid motion once the sliding mass rushed into the water. The RNG turbulent model is derived from rigorous statistical analyses, and it uses equations similar to the k-ε model. Empirical values are used for the equation constants (Lindsey et al. 2013).

The field investigation results and the hydrogeological data were used to establish the numerical model, and Fig. 12 shows the numerical model for the dynamic process of the landslide-generated wave from the Hongyanzi landslide. As shown in Fig. 12, the numerical model includes the following three parts: slope, sliding masses, and the Daning River. Cartesian coordinates were used for the numerical model in view of the specific configuration. Furthermore, in order to reduce the computational work, only a 540-m length of river was considered, and the still water level was assumed to be 145.0 m. The grid size was 10 m in all directions, and the model contains 382,320 cells in total. The following four monitoring points were set during the simulation process: point A (202, 300, and 145), point B (202, 500, and 145), point C (202, 900, and 145), and point D (202, 1500, and 145). Point A and point B are very close to the landslide area. Point C is located at the middle of the river, and point D is far from the landslide area, but the points are located in the same straight line (y direction).

Considering wave propagation problems, the symmetry boundary was set for the start face and end face of the computational domain in the x direction, and the specified pressure boundary (the air, free surface boundary) was set for the end face in the z direction. The other faces were set at the wall boundary, which means that the normal velocity there must be 0. The vertical gravity was applied to the entire system, and the acceleration of gravity was 9.8 m/s^2 in the negative z direction. The sliding masses were set as moving objects and scour material, and the initial state of the moving objects was motionless. After 150 s of calculation time for the fluid–solid coupled interacting model, the simulated results for the landslide-generated wave were obtained.

Formation of the wave

Once the landslide is initiated, the sliding masses form a semicircle wedge at the waterfront area and the surface morphology of the landslide tends to be a flow line. When the sliding masses rush into the river, the balance of the river is disturbed, and the water particles are vibrated. Figure 13 shows the simulated results for landslide-generated wave process in the main section. As shown in Fig. 13a, the landslide moves into the river valley as an integral rigid, and the movement of the sliding masses pushes and raises the river water. When the sliding masses occupied a part of the watercourse, the direction of the water movement was forward, downstream, and upstream, as shown in Fig. 13b. The motions of the water particles were stopped due to energy dissipation and resisting forces.

A landslide-generated wave generally contains two parts: (a) the volume-wave generated by the sliding masses along with the lifting of the water level and (b) the impulse-wave generated by the sliding masses entering the river at high speed. Landslide with the volume of 2.3×10^5 m^3 sliding into the Daning River at high-speed, huge potential energy is converted into the impulse-wave energy. Due to the relatively shallow watercourse and the wide river near the landslide site, it makes the volume-wave play the secondary

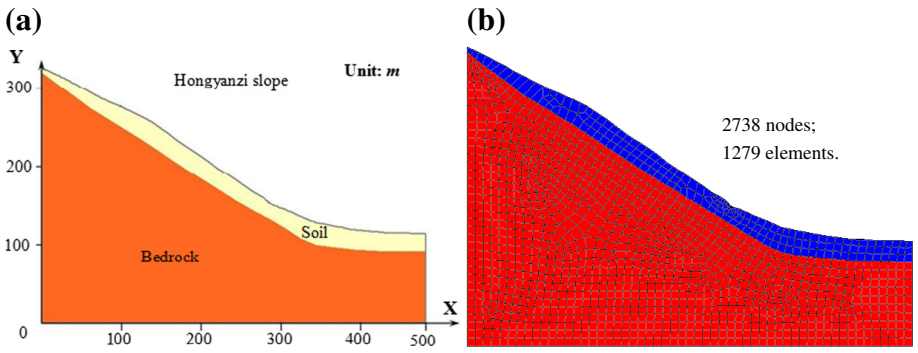

Fig. 8 Numerical modeling of the main section of the Hongyanzi slope, **a** geometry and geological conditions and **b** numerical mesh

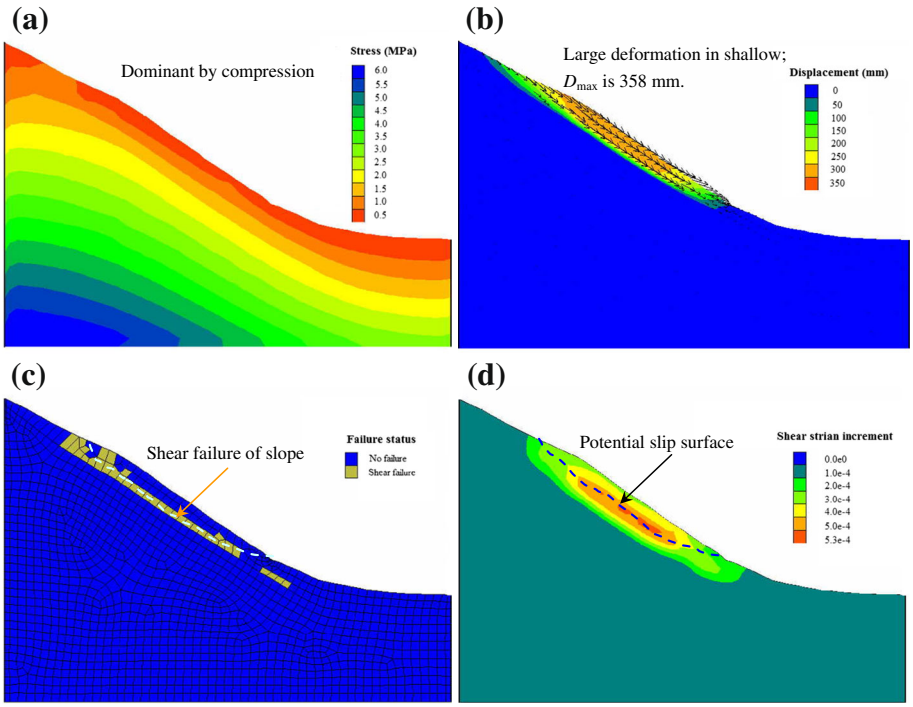

Fig. 9 Simulation results for the Hongyanzi slope under rainfall condition, **a** the first principal stress, **b** slope displacement distribution, **c** distribution of plastic zone, and **d** distribution of shear strain increment

role of the landslide-generated wave, and the impulse-wave is the dominant aspect. The wave was limited to the area around the sliding masses only at the beginning, because of the short-time landslide movement, and the peripheral water of the landslide was subject only to the friction force at the boundary of the water.

The dynamic process of the landslide-generated wave can be divided into three stages: (1) the beginning of the interaction between the sliding masses and the river water. Once the sliding masses rushed into the river, the water particles were pushed and expanded by the motion of the masses, which caused the free water surface to rise. The water tongue jumped to the water surface in a parabolic arc, and then, the lower water started to move from the static. The sliding masses splashed at the same time as the wave formation. (2) The formation of the wave along with the continuous falling of the sliding masses into the river caused a cavity to form at the tail of the sliding masses, and there were great difference inside and outside the cavity at the water level. The surrounding water moved into the cavity quickly and caused collisions, which produced a huge splash. At the same time, the energy carried by the sliding masses was transferred to the surrounding water and the wave formed. The largest height of the wave occurred in the landslide direction. The wave spread around in the form of a vibration wave with a small amount of water flow, which had the characteristics of the translation wave. (3) Wave propagation and attenuation. The wave height decayed gradually as it spreads around because of friction and energy dissipation.

Wave propagation process

The wave propagated around the interaction area of the sliding masses and the water surface. Figure 14 shows the evolution process for the elevation of the free surface at monitoring points A, B, C, and D in the y direction. As shown in Fig. 14, the water opposite the landslide began to fluctuate gently (point A), but at other points, it seemed still (point B, point C, and point D) in the early stage of sliding. After the landslide stopped, the water began to fluctuate turbulently, and it took the form of the water wave complex. The surface elevation rose after the landslide and then fell sharply, and it soon turned into an oscillation of small amplitude. The wave decayed gradually along with the spread of the energy, and the speed of the height attenuation gradually slowed after some sharp attenuation. In the stage of slow attenuation, the frictional resistance caused frictional head loss because of the relative velocity difference at the water surface. The maximum wave occurred 12 s after the end of the landslide ($t = 50$ s), and it formed near the leading edge of the main landslide profile. The maximum wave height was about 5.90 m at point A. About 67 s after the landslide stopped ($t = 105$ s), the water in point D flowed out. The maximum wave heights of the particles were in the course of propagation, and the fluctuating water level was above the original water level (elevation of 145 m) for the four monitoring points. The wave front was lower, with maximum wave heights of 3.95 m at point B, 3.12 m at point C, and 2.23 m at point D. The wave height is attenuation with a slower rate with the increasing of transmission distance.

Figure 13c shows the instantaneous free surface elevation and vectors of flow at 47 s after the Hongyanzi landslide. As shown in Fig. 13c, one peak of the wave was near the landslide area. All free surface elevations were higher than the original surface levels (elevation of 145 m), and the water level did not easily decrease

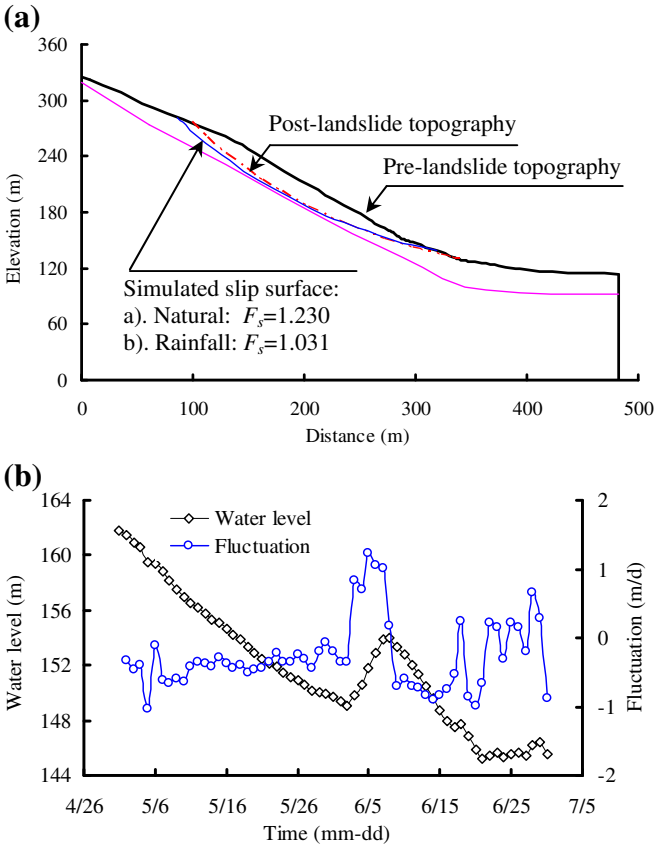

Fig. 10 **a** Critical slip surface and the corresponding safety factor of the Hongyanzi slope under natural and rainfall conditions, which were simulated by the limit equilibrium method and **b** monitoring results for the water level and corresponding fluctuation of the Three Gorges Reservoir at the Maoping hydrological point

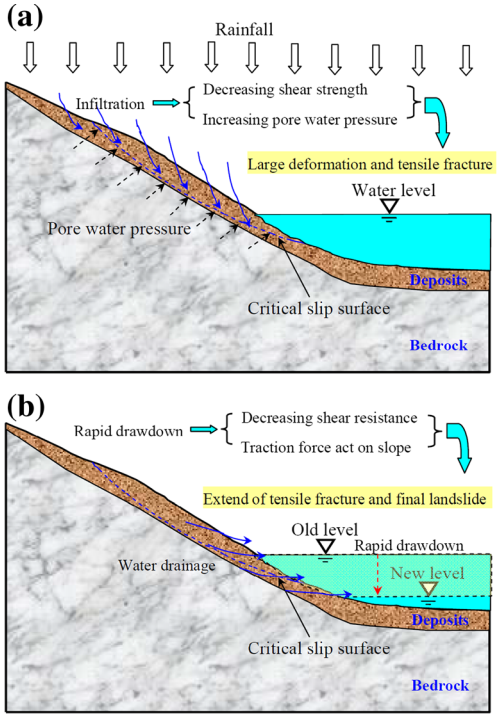

Fig. 11 Diagrams showing the initiation mechanism of the Hongyanzi landslide, **a** effect of rainfall on the slope and **b** effect of rapid drawdown of the water level on the slope

during the propagation. This phenomenon was very significant for the early warning and forecast during the landslide wave. The wave velocity is another important factor associated with early warning; it determines when and where the landslide-generated wave can arrive. The direction of the maximum velocity was consistent with the landslide direction and has the similar attenuation properties as the wave height. Finally, the wave decays gradually as it spreads due to friction and energy dissipation.

Once the landslide rushed into the river, the energy was transferred into the river water. The maximum kinetic energy of the landslide motion was about 3.49×10^{11} J when it crashed and stopped suddenly; this value was obtained by numerical calculation. Only small part of the kinetic energy of landslide will convert into the total energy of wave (about 3.37×10^{10} J). The solid–fluid energy conversion rate of the Hongyanzi landslide was about 9.66 %. During wave decay, the first half (propagating distance less than 500 m) was the rapid decay region in the river, and the decay rate was 0.9–1.2 %. This means that the wave decays 1 m after propagating 100 m. The other half (propagating distance greater than 500 m) is the gentle decay region, with a decay rate of 0.13–0.51 %. The decay is variable, not linear, and the wave decay is closely related to the hazardous range. Figure 15 shows the maximum height of the wave generated by the Hongyanzi landslide in the study region. As shown in Fig. 15, the maximum wave height occurred near the landslide, and the minimum wave height occurs on the opposite side. The first half of the wave decay is more rapid than the second half. The harmful range can be estimated coarsely based on the wave height, and the hazardous range of the wave generated by the landslide is larger than the landslide itself.

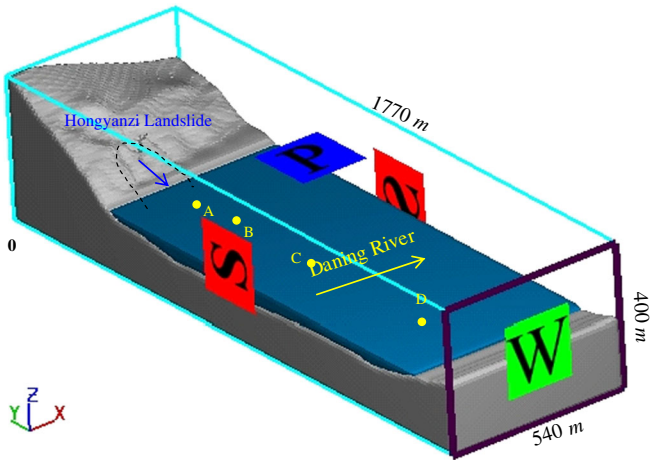

Fig. 12 Numerical model for the dynamic process of the landslide-generated wave caused by the Hongyanzi landslide. A, B, C, and D are four numerical monitoring points

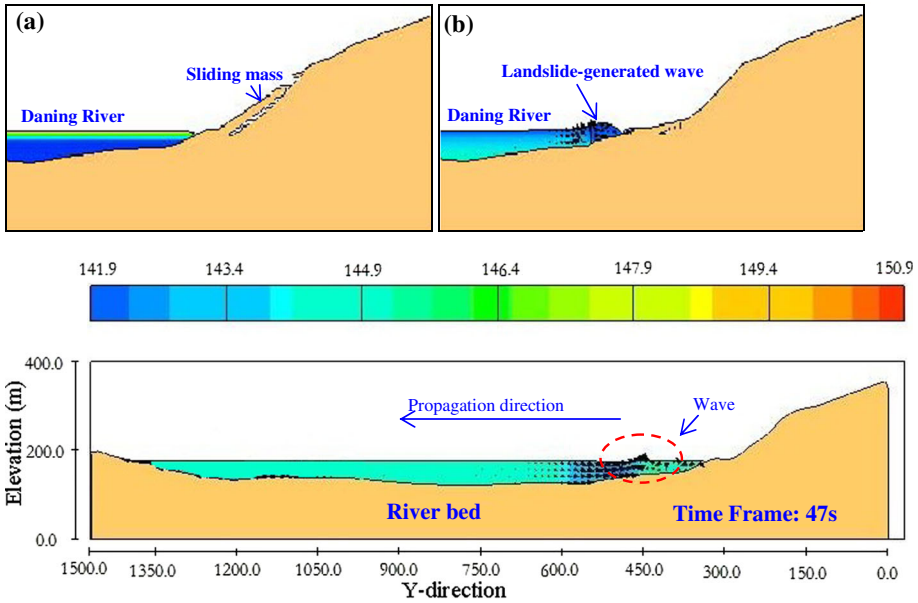

Fig. 13 Simulated results for landslide-generated wave process in the main section, **a** initial status, **b** interaction of water and sliding masses (the *arrows* represent the motion vector of the water particles), and **c** instantaneous free surface elevation and vectors of flow at 47 s after the Hongyanzi landslide

Discussions

Initiation mechanism of reservoir landslides

Landslides are one of the major geomorphological problems in reservoirs (Gutiérrez et al. 2015), especially in mountainous areas. Previous studies indicate that a large portion of the slope movements in reservoirs are related to the reactivation of pre-existing undetected landslides (Wang et al. 2007). New slope movements can occur upstream of a dam reservoir during the impoundment process because of varied groundwater levels along the upstream slope and saturation and softening of the slope soils below the water level (Schwab et al. 2004; Setiawan et al. 2015). For reservoir landslides, the fluctuation of the water level is the key triggering factor (Berilgen 2007). The reservoir bank slopes below the water level are affected by long-term saturation and flow erosion. Small failures happen on the lower slope, which is below the water level. Small failures at the toe of the slope do not have a great impact on the reservoir, but a free surface will form for the upper large volume of slope soils. This plays a key role in the following catastrophic reservoir landslide. The fluctuation of the water level includes two aspects, rising and drawdown, especially for rapid drawdown. The water-level fluctuations may induce changes in the pore water pressure in the bank slopes, which include seepage-induced pore pressures due to transient flow and stress-induced excess pore pressure (Yan et al. 2010; Vandamme and Zou 2013).

During the rapid drawdown process of reservoir water level, the descending speed of the slope internal saturation line lags behind

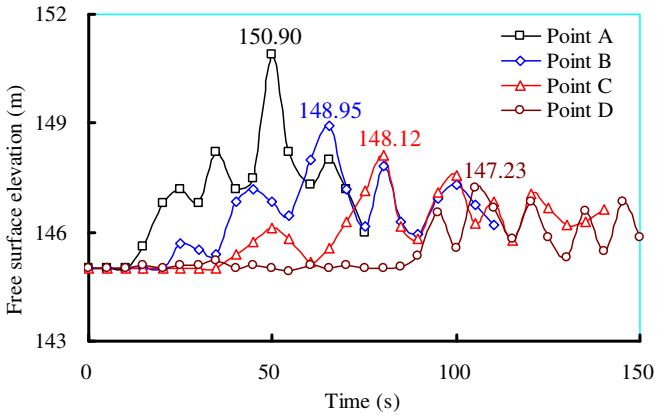

Fig. 14 Evolution of the elevation of the free surface at monitoring points A, B, C, and D in the *y* direction

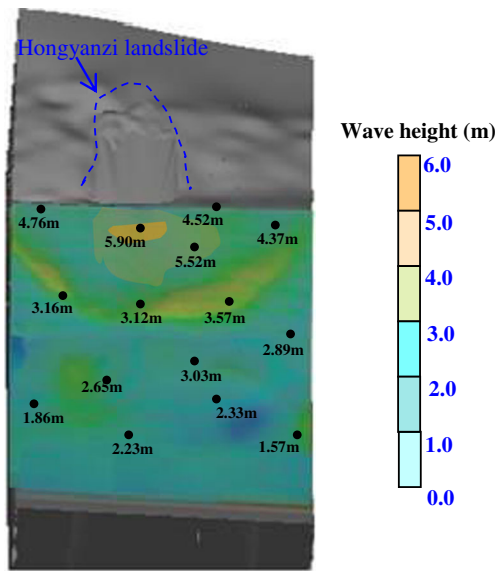

Fig. 15 Height of the wave generated by the Hongyanzi landslide in the study region

the drop speed of the slope outside water level, and the change in the external water level happens before the slope soils have time to drain (Wang and Qiao 2013). Dissipation of excess pore pressure and reduction of the seepage-induced pore pressure can cause traction force to act on the slope and decreased the slope stability, which may lead to the occurrence of a reservoir landslide (Zhang et al. 2012). Heavy or long-term rainfall is another important triggering factor for reservoir landslides (He et al. 2008). Rainfall infiltration can decrease the shear strength of slope soils and increase pore water pressure in the slope. When continuous rainfall occurs, a transient saturated zone is easily formed above the groundwater level, which can lead the loss of matric suction when the slope soil is saturated. This significantly reduces slope stability and may trigger failure of the bank slope. If rapid drawdown of the water level occurs at the same time, the coupling effect of rainfall and drawdown of the water level on the slope will cause a reservoir landslide to occur more easily. The Hongyanzi landslide is a typical example of this. In most cases, reservoir landslides are usually not triggered by a single factor (such as rainfall or a rising water level). Rather, they are the comprehensive responses to multiple factors affecting the reservoir slope.

For the Hongyanzi slope studied in this paper, the joint effect of intermittent rainfall and rapid drawdown of the water level resulted in the catastrophic reservoir landslide, and the dynamic process for the initiation of this landslide can be summarized in three stages: (1) intermittent rainfall cause the decreasing of shear strength of the soil and the increasing of pore water pressure in the slope, meanwhile tensile fractures are formed at the rear of the slope; (2) along with the intermittent rainfall and drawdown of the water level, a large deformation occurred, and the tensile fracture was further developed; a small local slide occurred at the toe of the slope; (3) the rainfall stopped, but the water level continued to decline. The shear resistance for the slope decreased, and the drainage of water in the slope caused the traction force to act on the shallow deposits. Finally, the result was the catastrophic landslide that happened on 24 June 2015.

Forecasting of landslide-generated wave

Once a large landslide is identified in a reservoir, the following two important questions should be answered: could this landslide lead to a hazardous impulse water wave, and what would be the scale of the landslide-generated wave (Gutiérrez et al. 2015)? The main factors affecting the landslide-generated wave include the volume and geometry of the landslide, its velocity of entry into the water, and the underwater topography of the reservoir (Panizzo et al. 2005; Ataie-Ashtiani and Yavari-Ramshe 2011). Although a landslide-generated wave is a typical secondary disaster of a reservoir landslide, the damage of the impulse water wave may be larger than that of the landslide itself. The effective forecasting of landslide-generated wave and prediction of its scale are very important for hazard prevention and mitigation of reservoir landslides. Usually, some empirical models are used to calculate the characteristic parameters of the landslide-generated wave. These models are usually used in engineering practice, and they can provide rapid evaluation for landslide-generated waves. Empirical models for the prediction of landslide-generated wave are well reviewed by Bornhold and Thomson (2012). However, most of the empirical models are presented from the laboratory test results, and assuming a certain proportion of potential energy is converted into the total energy of the waves (Bornhold et al. 2007). During the forecasting process of landslide-generated wave using empirical model, reasonable empirical model and computational parameters should be carefully selected according to the failure type and characteristics of the landslide; if not, large error may be existed.

Numerical models used for simulation of landslide-generated wave main include rigid body models, viscous flow models, Bingham plastic slide models, impulse wave models, and others. Comparisons of rigid body and viscous slide models show that the former generate much higher waves than the latter for the same input parameters (Bornhold and Thomson 2012). There are also significant differences in the propagation, frequency content and decay of landslide-generated wave by the two models (Bornhold and Thomson 2012). These differences are also existed in other type of numerical models, which mean that each type of numerical models has its own characteristics and scope of application. For the simulation of landslide-generated wave using numerical methods, reasonable numerical model and parameters should be used, same as the empirical methods. According to the forecasting of the landslide-generated wave, the empirical formula can be preliminary used to evaluate the characteristics of the wave. If the scale of the landslide-generated wave is small and it has no influence on the surrounding infrastructures and human beings, no further in-depth analysis is needed. However, if the empirical formula predicts that the scale of the wave is large enough to cause destruction or damage to the surrounding infrastructure and endanger people, then numerical methods can be used to simulate the propagation process of the wave in detail.

Conclusions

The initiation of reservoir landslides is generally related to the fluctuation of the water level and rainfall duration in the reservoir area. Once the sliding masses of the reservoir landslide suddenly rush into the river, a wave is generated, and it can pose a great threat to the surrounding residents and their buildings and ships. Studies of the triggering conditions and mechanism of the landslide-generated wave process are very important for hazard prevention and mitigation of reservoir landslides. In this paper, the 24 June 2015 Hongyanzi landslide at the Three Gorges Reservoir was used as an example to study the initiation mechanism of a landslide-generated wave from a reservoir landslide.

The finite difference method and limit equilibrium analysis were used to analyze the deformation and failure characteristics of the Hongyanzi slope. Simulation results show that a large deformation (about 358 mm) happened in the shallow deposits under intermittent rainfall condition, and a clear potential slip surface formed in the Hongyanzi slope. The safety factor of the Hongyanzi slope under natural condition is 1.230, and it decreased to 1.031 under rainfall condition, which means that the slope reached the limit state after antecedent intermittent rainfall duration. From 8 June 2015 to 24 June 2015, the water level of Three Gorges decline rapidly, at a rate of −0.55 m/day. The rapid drawdown of the water level reduced the support for the Hongyanzi slope, and it accelerated the drainage of water from the slope, which provided the dynamic conditions for the initiation of the landslide. Thus, the initiation of the Hongyanzi landslide was the result of multiple influences, including the intermittent rainfall

and the rapid drawdown of the water level for the reservoir deposit slope.

Numerical methods were used to simulate the landslide-generated wave process of the Hongyanzi landslide. The results show that, when the sliding masses rush into the river, the balance of the river is disturbed and the water particles are vibrated. The landslide wave is dominated by the impact wave generated by the sliding masses entering the river at high speed. The maximum wave height of 5.90 m occurs near the landslide (it occurred 12 s after the end of the landslide), and the minimum wave height occurs on the opposite side. The direction of the maximum velocity is consistent with the landslide direction. Finally, the wave decays gradually as it spreads, due to friction and energy dissipation. For the prevention of reservoir landslides, the most important point is that the speed of increase or drawdown of the water level should be controlled. Rapid fluctuations of the water level need to be avoided, especially for drawdown. Also, rainfall infiltration into the slope should be reduced by engineering and non-engineering measures, such as maintaining good vegetation cover, promoting ecological protection, and installing an impermeable membrane cover for the slope. Furthermore, some drainage measures can be adopted for the slope to accelerate the drainage of infiltrated water; drainage holes can be used, for example. For the forecasting of a landslide-generated wave, some empirical formulas can be preliminarily used to evaluate the characteristics of the wave. If the scale of the landslide-generated wave is large enough, then numerical methods can be used to simulate the propagation of the wave in detail. However, for some potential catastrophic reservoir landslides, engineering measures cannot prevent the landslide. In these cases, some mitigation measures should be planned ahead of time, such as relocation of residents and prohibition of navigation.

Acknowledgments

We gratefully acknowledge the support of the National Natural Science Foundation of China (41472272 and 41102194) and the Science Foundation for Excellent Youth Scholars of Sichuan University (2013SCU04A07). Critical comments by anonymous reviewers greatly improved the initial manuscript.

References

Abadie S, Morichon D, Grilli S, Glockner S (2010) Numerical simulation of waves generated by landslides using a multiple-fluid Navier–Stokes model. Coast Eng 57:779–794

Aleotti P, Chowdhury R (1999) Landslide hazard assessment: summary review and new perspectives. Bull Eng Geol Environ 58:21–44

Ataie-Ashtiani B, Mansour-Rezaei S (2009) Modification of weakly compressible smoothed particle hydrodynamics for preservation of angular momentum in simulation of impulsive wave problems. Coast Eng J 51:363–386

Ataie-Ashtiani B, Yavari-Ramshe S (2011) Numerical simulation of wave generated by landslide incidents in dam reservoirs. Landslides 8:417–432

Berilgen MM (2007) Investigation of stability of slopes under drawdown conditions. Comput Geotech 34:81–91

Bornhold BD, Thomson RE (2012) Tsunami hazard assessment related to slope failures in coastal waters. In: Clague JJ, Stead D (eds) Landslides: types, mechanisms, and modelling. Cambridge University Press, New York, pp 108–120

Bornhold BD, Harper JR, McLaren D, Thomson RE (2007) Destruction of the First Nations village of Kwalate by a rock avalanche-generated tsunami. Atmosphere-Ocean 45:123–128

Bosa S, Petti M (2011) Shallow water numerical model of the wave generated by the Vajont landslide. Environ Model Softw 26:406–418

Choi BH, Pelinovsky E, Kim DC, Didenkulova I, Woo SB (2008) Two- and three-dimensional computation of solitary wave runup on non-plane beach. Nonlinear Process Geophys 15:489–502

Chopakatla SC, Lippmann TC, Richardson JE (2008) Field verification of a computational fluid dynamics model for wave transformation and breaking in the surf zone. J Waterw Port Coast Ocean Eng 134:71–80

Chung CJF, Fabbri AG (1999) Probabilistic prediction models for landslide hazard mapping. Photogramm Eng Remote Sens 65:1389–1399

Das K, Green S, Basu D, Janetzke R, Stamatakos J (2009) Effect of slide deformation and geometry on waves generated by submarine landslides: a numerical investigation. Offshore Technology Conference, Texas, pp 1–12

Duc DM (2013) Rainfall-triggered large landslides on 15 December 2005 in Van Canh District, Binh Dinh Province, Vietnam. Landslides 10:219–230

Fritz HM, Hager WH, Minor HE (2004) Near field characteristics of landslide generated impulse waves. J Waterw Port Coast Ocean Eng 130:287–302

Gutiérrez F, Linares R, Roqué C, Zarroca M, Carbonel D, Rosell J, Gutiérrez M (2015) Large landslides associated with a diapiric fold in Canelles Reservoir (Spanish Pyrenees): detailed geological-geomorphological mapping, trenching and electrical resistivity imaging. Geomorphology 241:224–242

Guzzetti F, Carrara A, Cardinali M, Reichenbach P (1999) Landslide hazard evaluation: a review of current techniques and their application in a multi-scale study, central Italy. Geomorphology 31:181–216

He KQ, Li XR, Yan XQ, Guo D (2008) The landslides in the Three Gorges Reservoir region, China and the effects of water storage and rain on their stability. Environ Geol 55:55–63He KQ, Wang SQ, Du W, Wang SJ (2010) Dynamic features and effects of rainfall on landslides in the Three Gorges Reservoir region, China: using the Xintan landslide and the large Huangya landslide as the examples. Environ Earth Sci 59:1267–1274

Hu XL, Zhang M, Sun MJ, Huang KX, Song YJ (2015) Deformation characteristics and failure mode of the Zhujiadian landslide in the Three Gorges Reservoir, China. Bull Eng Geol Environ 74:1–12

Huang BL, Zheng WJ, Yu ZZ, Liu GN (2014) A successful case of emergency landslide response—the Shanshucao landslide, Three Gorges Reservoir, China. Geoenviron Disaster 2:18

Iverson RM (2000) Landslide triggering by rain infiltration. Water Resour Res 36:1897–1910

Jiang JW, Xiang W, Rohn J, Zeng W, Schleier M (2015) Research on water–rock (soil) interaction by dynamic tracing method for Huangtupo landslide, Three Gorges Reservoir, PR China. Environ Earth Sci 74:557–571

Koo W, Kim MH (2008) Numerical modeling and analysis of waves induced by submerged and aerial-sub-aerial landslides. KSCE J Civ Eng 12:77–83

Lindsey AL, Jasim IM, Hanif C (2013) 3D numerical simulation of partial breach dam-break flow using the LES and k–ε turbulence models. J Hydraul Res 51:145–157

Liu JG, Mason PJ, Clerici N, Chen S, Davis A, Miao F, Liang L (2004) Landslide hazard assessment in the Three Gorges area of the Yangtze River using ASTER imagery: Zigui-Badong. Geomorphology 61:171–187

Montagna F, Bellotti G, Risio MD (2011) 3D numerical modeling of landslide-generated tsunamis around a conical island. Nat Hazards 58:591–608

Panizzo A, De Girolamo P, Di Risio M, Maistri A, Petaccia A (2005) Great landslide events in Italian artificial reservoirs. Nat Hazards Earth Syst Sci 5:733–740

Pastor M, Herreros I, Merodo JF, Mira P, Haddad B, Quecedo M, Drempetic V (2009) Modelling of fast catastrophic landslides and impulse waves induced by them in fjords, lakes and reservoirs. Eng Geol 109:124–134

Saito Y, Yang Z, Hori K (2001) The Huanghe (Yellow River) and Changjiang (Yangtze River) deltas: a review on their characteristics, evolution and sediment discharge during the Holocene. Geomorphology 41:219–231

Schwab JW, Geertsema M, Blais-Stevens A (2004) The Khyex River landslide of November 28, 2003, Prince Rupert British Columbia Canada. Landslides 1:243–246

Setiawan H, Takara K, Sassa K, Miyagi T (2015) Shear strength reduction in progress of shear displacement on the landslide near dam reservoir. Proc Environ Sci 28:587–594

Tang HM, Li CD, Hu XL, Su AJ, Wang LQ, Wu YP, Criss R, Xiong CR, Li YN (2015) Evolution characteristics of the Huangtupo landslide based on in situ tunneling and monitoring. Landslides 12:511–521

Vandamme J, Zou QP (2013) Investigation of slope instability induced by seepage and erosion by a particle method. Comput Geotech 48:9–20

Wang M, Qiao JP (2013) Reservoir-landslide hazard assessment based on GIS: a case study in Wanzhou section of the Three Gorges Reservoir. J Mt Sci 10:1085–1096
Wang FW, Zhang YM, Huo ZT, Matsumoto T, Huang B (2004) The July 14, 2003 Qianjiangping landslide, Three Gorges Reservoir, China. Landslides 1:157–162
Wang HB, Xu WY, Xu RC, Jiang QH, Liu JH (2007) Hazard assessment by 3D stability analysis of landslides due to reservoir impounding. Landslides 4:381–388
Wu SR, Jin YM, Zhang YS, Shi JS, Dong C, Lei WZ, Shi L, Tang CX, Hu D (2004) Investigations and assessment of the landslide hazards of Fengdu County in the reservoir region of the Three Gorges project on the Yangtze River. Environ Geol 45:560–566
Xu FG, Yang XG, Zhou JW (2015a) Experimental study of the impact factors of natural dam failure introduced by a landslide wave. Environ Earth Sci 74:4075–4087
Xu FG, Yang XG, Zhou JW (2015b) A mathematical model for determining the maximum impact stress on a downstream structure induced by dam-break flow in mountain rivers. Arab J Geosci 8:4541–4553
Yan ZL, Wang JJ, Chai HJ (2010) Influence of water level fluctuation on phreatic line in silty soil model slope. Eng Geol 113:90–98
Yavari-Ramshe S, Ataie-Ashtiani B (2015) A rigorous finite volume model to simulate subaerial and submarine landslide-generated waves. Landslides. doi:10.1007/s10346-015-0662-6
Yin H, Li C (2001) Human impact on floods and flood disasters on the Yangtze River. Geomorphology 41:105–109
Yin KL, Liu YL, Wang Y, Jiang ZB (2012) Physical model experiments of landslide-induced wave in Three Gorges Reservoir. J China Univ Geosci 37:1067–1074 **(in Chinese)**
Yin YP, Huang BL, Chen XT, Liu G, Wang S (2015) Numerical analysis on wave generated by the Qianjiangping landslide in Three Gorges Reservoir, China. Landslides 12:355–364
Zhang MS, Dong Y, Sun PP (2012) Impact of reservoir impoundment-caused groundwater level changes on regional slope stability: a case study in the Loess Plateau of Western China. Environ Earth Sci 66:1715–1725
Zhou JW, Xu WY, Yang XG, Shi C, Yang ZH (2010) The 28 October 1996 landslide and analysis of the stability of the current Huashiban slope at the Liangjiaren Hydropower Station, Southwest China. Eng Geol 114:45–56
Zhou JW, Cui P, Yang XG, Su ZM, Guo XJ (2013) Debris flows introduced in landslide deposits under rainfall conditions: the case of Wenjiagou gully. J Mt Sci 10:249–260
Zhou JW, Cui P, Hao MH (2016a) Comprehensive analyses of the initiation and entrainment processes of the 2000 Yigong catastrophic landslide in Tibet, China. Landslides 13:39–54
Zhou JW, Cui P, Yang XG (2016b) Effects of material composition and water content on the mechanical properties of landslide deposits triggered by the Wenchuan earthquake. Acta Geol Sin 90:242–257, **English Edition**

J. Zhou (✉) · F. Xu · X. Yang
State Key Laboratory of Hydraulics and Mountain River Engineering,
Sichuan University,
Chengdu, 610065, People's Republic of China
e-mail: jwzhou@scu.edu.cn

Y. Yang · P. Lu
College of Water Resource and Hydropower,
Sichuan University,
Chengdu, 610065, People's Republic of China